Equation of state and sound velocity of a hadronic gas with a hard-core interaction

L. M. Satarov,[1,2] K. A. Bugaev,[1,3] and I. N. Mishustin[1,2]
[1]*Frankfurt Institute for Advanced Studies, D-60438 Frankfurt am Main, Germany*
[2]*National Research Center "Kurchatov Institute," 123182 Moscow, Russia*
[3]*Bogolyubov Institute for Theoretical Physics, 03680 Kiev, Ukraine*
(Received 5 November 2014; revised manuscript received 24 March 2015; published 15 May 2015)

Thermodynamic properties of hot and dense hadronic systems with a hard-sphere interaction are calculated in the Boltzmann approximation. Two parametrizations of pressure as a function of density are considered: the first one, used in the excluded-volume model and the second one, suggested earlier by Carnahan and Starling. The results are given for one-component systems containing only nucleons or pions, as well as for chemically equilibrated mixtures of different hadronic species. It is shown that the Carnahan–Starling approach can be used in a much broader range of hadronic densities as compared to the excluded-volume model. In this case the superluminal sound velocities appear only at very high densities, in the region where the deconfinement effects should be already important.

DOI: 10.1103/PhysRevC.91.055203 PACS number(s): 21.65.Mn, 25.75.−q, 21.30.Fe

I. INTRODUCTION

Physics of strongly interacting matter under extreme conditions is in the focus of research in several fields including relativistic heavy-ion collisions, compact stars, and the early universe. In recent years, significant progress was achieved in lattice calculations of the equation of state (EoS) at high temperatures and low baryon densities. However, the lattice approach cannot be used reliably at low temperatures and high baryon densities. The information on the EoS in this domain remains a subject of model calculations. It is obvious that realistic calculations of the EoS of dense hadronic systems should take into account a strong interaction between hadrons.

A hard-sphere interaction (HSI) is one of the most popular methods to implement short-range repulsion effects for calculating thermodynamic properties of multiparticle systems. In this approach the particles of a sort i are represented by hard spheres of radius R_i. It is assumed that particles move freely unless the distance r_{ij} between centers of any pair i,j becomes equal to $R_i + R_j$. It is postulated that the potential energy of an ij interaction is infinite at smaller r_{ij}. Originally such an approximation was suggested by van der Waals [1] to describe properties of dense gases and liquids. Later on the HSI-based models were successfully used by many authors in condensed matter physics [2,3]. A similar approach, the so-called excluded-volume model (EVM), was applied in Refs. [4–11] to describe the EoS of hot and dense hadronic matter. These studies revealed a very strong sensitivity of the EoS to parameters of the short-range repulsion between hadrons. In particular, it was shown in Refs. [5–7] that a reasonable phase diagram of strongly interacting matter can only be obtained after accounting for the finite size of hadrons. Our present study is aimed at a more realistic description of the HSI effects in the hadronic EoS.

Unfortunately, the van der Waals approach is essentially nonrelativistic. As a consequence, it cannot be safely applied when the sound velocity of matter c_s becomes comparable with the light velocity. It is well known that the EVM violates the casuality condition[1] $c_s < 1$ at sufficiently high baryon densities [7]. Attempts to remove this drawback were made in Refs. [8,12] (see also Refs. [13,14]). Moreover, it will be shown below that the EVM becomes inaccurate at high densities when the total volume of constituents exceeds 10%–20% of the system volume. By comparing with the virial expansion [2,15] one may conclude that this model overestimates the contribution of nonbinary interactions to pressure.

On the other hand, numerical simulations of one-component liquids with HSI show [2] that the Carnahan–Starling approximation (CSA) of pressure [16] successfully works up to much higher densities than in the EVM. Below we use the CSA and EVM to calculate properties of thermodynamically equilibrated hadronic systems containing mesons and (anti)baryons.[2] An important feature of such systems is that partial numbers of different species $\pi, N, \Delta, \ldots$ are, in general, not conserved due to presence of inelastic processes and resonance decays. These numbers are not independent and should be determined from the conditions of chemical equilibrium [7].

Up to now information about properties of multicomponent systems with HSI is rather scarce [3]. In this paper we consider several representative cases: first, we study the $N + \Delta$ and $\pi + N + \Delta$ mixtures with equal sizes of all hadrons and second, the $\pi + N + \Delta$ system assuming that baryons have equal radii, $R_\Delta = R_N$, and pions are point like, $R_\pi = 0$.[3] Finally, we make calculations for hadronic systems with an extended set of baryons, antibaryons, and mesons. The main emphasis is given to calculating the sound velocity. According

[1]Units $\hbar = c = 1$ are used throughout the paper.
[2]For simplicity, we disregard the isospin and Coulomb effects and neglect nonzero widths of resonances.
[3]Note that small [10] or even vanishing [11] pion radii are favored by recent fits of hadron multiplicities measured in central heavy-ion collisions at the AGS, SPS, and RHIC bombarding energies.

to our analysis, the CSA predicts a much softer EoS, with smaller c_s values than in the EVM. Choosing reasonable values of hadronic radii, we show that acausal states in the CSA are shifted to baryon densities $n_B \gtrsim 1$ fm^{-3}. It is expected that at such densities the deconfinement effects, in particular, the formation of a quark-gluon phase, should already be important.

The paper is organized as follows: In Sec. II we consider one-component systems with hard-sphere particles. First we introduce parametrizations of pressure in the EVM and CSA. Then we calculate properties of an ideal gas in the Boltzmann approximation. Analytic expressions for shifts of thermodynamic functions due to HSI are obtained in Secs. II C and II D. The EoS and sound velocities of nucleonic and pion matter are analyzed in Secs. II D and II E. In Sec. III we study properties of hadronic mixtures. In the end of this section we discuss the importance of quantum-statistical corrections. The summary and outlook are given in Sec. IV.

II. ONE-COMPONENT HADRONIC SYSTEMS

A. Compressibility and virial expansion

In this section we consider a one-component system containing only one sort of hard-sphere particles with radius R. Below we disregard the effects of Fermi or Bose statistics i.e., all calculations are done in the classical (Boltzmann) approximation (the accuracy of this approximation will be discussed in Sec. III F). In this case one can write the following expression for pressure as a function of temperature and particle density $n = N/V$ [2,3]:

$$P = nT\,Z(n) = P_{\rm id} Z(n). \tag{1}$$

Here $P_{\rm id}$ is the ideal-gas pressure and Z is the "compressibility" factor, which depends only on the dimensionless "packing" fraction $\eta = nv$ where $v = 4\pi R^3/3$ is the proper volume of a single particle. At small η one can use a universal virial expansion [2]

$$Z = 1 + 4\eta + 10\eta^2 + \cdots . \tag{2}$$

This expansion is not applicable[4] for η exceeding about 0.5. Equation (2) may be applied to estimate the accuracy of EoS calculations for multiparticle systems with HSI.

Instead of Eq. (2), different analytical approximations for Z are used by many authors. For example, the following van der Waals-motivated parametrization is used in the EVM:

$$Z_{\rm EVM} = \frac{1}{1-4\eta}. \tag{3}$$

One can see that such an ansatz leads to inaccurate results at sufficiently high η. Indeed, comparison of the right-hand side (r.h.s.) of Eq. (3), decomposed in powers of η, with Eq. (2) shows that only first two terms of the virial expansion are correctly reproduced in the EVM. It is clear that densities $n > 0.25/v$ cannot be reached in this model due to the divergence of pressure at $\eta = 0.25$. As demonstrated in Ref. [7], the EVM leads to superluminal sound velocities already at $\eta \gtrsim 0.2$. This is a consequence of a too stiff density dependence of pressure assumed in this model.

On the other hand, the Carnahan–Starling parametrization [16]

$$Z_{\rm CSA} = \frac{1+\eta+\eta^2-\eta^3}{(1-\eta)^3} \tag{4}$$

is able to reproduce rather accurately [2] the first eight terms of the virial expansion for $Z(n)$. It agrees well with numerical calculations at $\eta \lesssim 0.5$, i.e., up to the boundary of liquid phase. Note that both above-mentioned parametrizations give similar results in the region $\eta \ll 1$ where $Z \simeq 1 + 4\eta$. This is illustrated in Fig. 1. One can see that at $\eta \gtrsim 0.2$ the Carnahan–Starling EoS is indeed noticeably softer as compared with the EVM.

Equation (1) gives pressure as a function of canonical variables: temperature T and density n. As explained above, in the situation when particle densities are not fixed, more appropriate variables are temperature and chemical potential μ. It is possible to calculate other thermodynamic functions, in particular the energy and entropy densities, ε and s, if the dependence $\mu = \mu(T,n)$ is known. To get explicit expressions for these functions, it is convenient to calculate first the free-energy density $f = \mu n - P$ as a function of T and n. Then one can use thermodynamical identities [15]

$$\varepsilon = f + Ts, \quad s = -\left(\frac{\partial f}{\partial T}\right)_n . \tag{5}$$

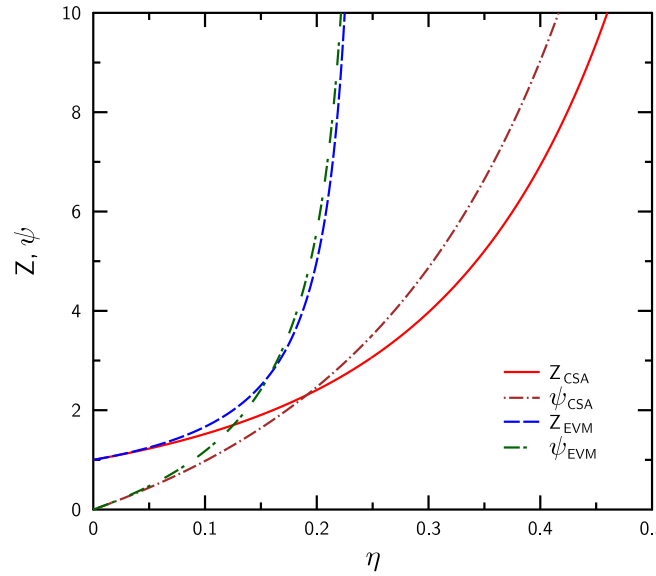

FIG. 1. (Color online) Compressibility factor Z and function ψ [see Eq. (21)] for different values of packing fraction η calculated within the EVM and CSA.

[4]The most dense state of the considered systems corresponds to the ordered (face-centered cubic) lattice with $\eta = \frac{\pi}{3\sqrt{2}} \simeq 0.74$. Direct Monte Carlo simulations show [3] that the liquid-solid phase transition in a one-component matter with HSI occurs in the interval $0.49 < \eta < 0.55$.

B. Thermodynamic functions of ideal gas

Let us start by calculating thermodynamic functions of an ideal gas of particles with the mass m and the spin-isospin degeneracy factor g. In the Boltzmann approximation one can write down [7] the equation relating the particle density and the chemical potential:

$$n = \phi(T)\exp\left(\frac{\mu_{\rm id}}{T}\right), \quad \phi(T) \equiv \frac{gm^3}{2\pi^2}\frac{K_2(x)}{x}. \tag{6}$$

Here $x = m/T$, $K_n(x)$ is the McDonald function of nth order, and the subscript "id" implies the ideal-gas limit. The function ϕ has the meaning of the ideal-gas density in the case of zero chemical potential.

From Eq. (6) and formulas of preceding section we get the following expressions for thermodynamic functions of the ideal gas:

$$\mu_{\rm id} = T\ln\frac{n}{\phi(T)}, \tag{7}$$

$$f_{\rm id} = \mu_{\rm id}n - P_{\rm id} = nT\left[\ln\frac{n}{\phi(T)} - 1\right], \tag{8}$$

$$s_{\rm id} = n\left[\ln\frac{\phi(T)}{n} + \xi(T)\right], \tag{9}$$

$$\varepsilon_{\rm id} = nT[\xi(T) - 1], \tag{10}$$

where

$$\xi(T) = T\frac{\phi'(T)}{\phi(T)} + 1 = x\frac{K_3(x)}{K_2(x)}. \tag{11}$$

Unless otherwise stated, we denote by prime the derivative with respect to T. According to Eq. (10), in the ideal-gas limit, the heat capacity per particle $\widetilde{C} = n^{-1}(\frac{\partial\varepsilon}{\partial T})_n$ is a function of temperature only:

$$\widetilde{C} = [T(\xi - 1)]' = x^2 + 3\xi - (\xi - 1)^2. \tag{12}$$

The sound velocity is an important characteristic of EoS which gives the propagation speed of small density perturbations in the matter rest frame. In absence of dissipation the adiabatic sound velocity squared is equal to [17]

$$c_s^2 = \left(\frac{\partial P}{\partial\varepsilon}\right)_\sigma, \tag{13}$$

where the subscript σ in the r.h.s. means that the derivative is taken along the Poisson adiabat, i.e., at constant entropy per particle:[5] $\sigma = s/n = \text{const}$. One can rewrite Eq. (13) in the form

$$c_s^2 = \frac{(\partial P/\partial n)_T + (\partial P/\partial T)_n(\partial T/\partial n)_\sigma}{(\partial\varepsilon/\partial n)_T + (\partial\varepsilon/\partial T)_n(\partial T/\partial n)_\sigma}. \tag{14}$$

Using Eqs. (9), (12), and the relation $d\sigma = dn\,\partial\sigma/\partial n + dT\,\partial\sigma/\partial T = 0$ we get in the ideal-gas limit

$$n\left(\frac{\partial T}{\partial n}\right)_\sigma = \frac{T}{\widetilde{C}}. \tag{15}$$

After calculating the derivatives of P,ε in (14) and using Eq. (15) we obtain the following formula for the sound velocity of a one-component ideal gas:

$$c_s^{\rm id} = \sqrt{\xi^{-1}(1 + \widetilde{C}^{-1})}. \tag{16}$$

One can see that the sound velocity of the classical ideal gas is a function of temperature only.

In the nonrelativistic limit, $T \ll m$, using the asymptotic formulas for McDonald functions, one gets the approximate expressions

$$\xi \simeq x + \frac{5}{2} + \frac{15}{8x} + \cdots, \quad \widetilde{C} \simeq \frac{3}{2} + \frac{15}{4x} - \frac{15}{2x^2} + \cdots. \tag{17}$$

Substituting Eq. (17) into Eq. (16), we get the well-known nonrelativistic expression $c_s^{\rm id} \simeq \sqrt{\frac{5T}{3m}}$ for the sound velocity of a monatomic ideal gas.

In the opposite, high-temperature limit, $T \gg m$, one obtains from Eqs. (11)–(12)

$$\xi \simeq 4 + \frac{x^2}{2} + \cdots, \quad \widetilde{C} \simeq 3 - \frac{x^2}{2} + \cdots. \tag{18}$$

This leads to the ultrarelativistic result $c_s^{\rm id} \simeq 1/\sqrt{3} \simeq 0.577$. One can show that $c_s^{\rm id}(T)$ is a monotonically increasing function with the asymptotic value $1/\sqrt{3}$.

C. Contribution of hard-sphere interaction

In this section we consider deviations from the ideal-gas limit for particles with HSI. Let us denote by ΔA the shift of any quantity from its ideal-gas value:

$$\Delta A \equiv A - A_{\rm id}. \tag{19}$$

It is clear that $\Delta A \to 0$ in the dilute gas limit $n \to 0$. Integrating the thermodynamic relation [15] $d\mu = \frac{1}{n}(dP - sdT)$ along the density axis (at fixed T), one obtains the equation

$$\Delta\mu(T,n) = \int_0^n \frac{dn_1}{n_1}\frac{\partial\Delta P(T,n_1)}{\partial n_1}. \tag{20}$$

Here we have used the condition $\lim_{n\to 0}\Delta\mu = 0$. Substituting $\Delta P = nT(Z - 1)$, one arrives at the relation $\Delta\mu = T\psi(n)$ where

$$\psi(n) = Z(n) - 1 + \int_0^n \frac{dn_1}{n_1}[Z(n_1) - 1]. \tag{21}$$

The same formula for $\Delta\mu$ has been obtained earlier in Ref. [18]. Using further Eq. (7) we finally get the equation for the chemical potential $\mu = \mu_{\rm id} + \Delta\mu$ as a function of T and n:

$$\mu = T\left[\ln\frac{n}{\phi(T)} + \psi(n)\right]. \tag{22}$$

By solving Eq. (22) with respect to n and substituting the result into Eq. (1) one can calculate pressure as a function of grand-canonical variables T,μ. In particular, this may be useful for finding possible phase transitions by using the Gibbs construction. Parametrizations of the compressibility factor introduced in Sec. II A are rather useful because they permit an analytical integration in Eq. (21). For example, in the EVM

[5] In a general case, when particle numbers are not conserved, σ equals the entropy per baryon.

Eqs. (1), (3), and (21) give the following result:

$$\psi_{\rm EVM} = Z - 1 + \ln Z = \frac{bP}{T} + \ln\left(1 + \frac{bP}{T}\right), \qquad (23)$$

where $b = 4v$ is the "excluded volume" introduced by van der Waals. Substituting Eq. (23) into Eq. (22) leads to a simple formula for chemical potential:

$$\mu = T \ln \frac{P}{T\phi(T)} + bP \quad \text{(EVM)}. \qquad (24)$$

One can regard Eq. (24) as the implicit equation for $P = P(T,\mu)$. In the case considered, solving Eq. (24) with respect to P is equivalent to solving Eq. (22) with respect to n. It is worth noting that, in the EVM, the shift of chemical potential from the ideal-gas value ($b = 0$) is linear in pressure. But this conclusion is not universal: it does not hold in the CSA.

Indeed, substituting (4) into Eq. (21) gives the following formula:

$$\psi_{\rm CSA} = \frac{3-\eta}{(1-\eta)^3} - 3. \qquad (25)$$

In Fig. 1 we present numerical values of $\psi(n)$ in the EVM and CSA. One can see that at given T,n the values of ψ and, therefore, deviations of chemical potential from the ideal-gas values are larger in the EVM.

D. Nucleonic matter

Let us consider first a system consisting of nucleons ($m = 939$ MeV, $g = 4$). In this case n is the conserved baryon density, which together with temperature defines the thermodynamic state. At fixed n and T the shift of free-energy density due to nucleon interactions equals $\Delta f = n\Delta\mu - \Delta P$. Using further Eqs. (8) and (21) we obtain the expression for the free-energy density of interacting nucleons,

$$f = nT\left\{\ln\frac{n}{\phi(T)} - 1 + \int_0^n \frac{dn_1}{n_1}[Z(n_1) - 1]\right\}. \qquad (26)$$

Equations (5) and (26) lead to the following formulas for entropy and energy densities:

$$s = n\left\{\ln\frac{\phi(T)}{n} + \xi(T) - \int_0^n \frac{dn_1}{n_1}[Z(n_1) - 1]\right\}, \qquad (27)$$

$$\varepsilon = f + Ts = nT[\xi(T) - 1], \qquad (28)$$

where $\xi(T)$ is defined in Eq. (11).

From Eqs. (10) and (28) one can see that HSI does not produce any shift of the energy density as compared to the ideal gas of point-like nucleons.[6] As a consequence, the isochoric heat capacity $C_{\rm V} = (\partial\varepsilon/\partial T)_n$ is the same as in the ideal gas: $C_{\rm V} = n\widetilde{C}(T)$ where $\widetilde{C}(T)$ is given by Eq. (12). According to Eq. (27), the entropy per particle $\sigma = s/n$ is reduced due to hard-core interaction of nucleons. This leads to a modification of the Poisson adiabat ($\sigma = $ const) in the n-T plane as compared to the ideal gas. Indeed, using Eq. (27), we obtain for the isentropic process,

$$n\left(\frac{\partial T}{\partial n}\right)_\sigma = ZT\widetilde{C}^{-1}. \qquad (29)$$

Comparing this result with Eq. (15) we conclude that the slope of the Poisson adiabat of nucleonic matter increases with density due to the appearance of the compressibility factor $Z > 1$.

The sound velocity can be obtained from Eqs. (1), (14), and (28)–(29). This leads to the analytical expression

$$c_s^2 = \frac{1}{\xi + Z - 1}[(nZ)' + Z^2\widetilde{C}^{-1}], \qquad (30)$$

where prime means the derivative with respect to n. In the ideal-gas limit $Z \to 1$ this formula coincides with Eq. (16). In the case of a nucleon gas at realistic temperatures $T \ll m$, using the relations (17) one can derive the approximate formula

$$c_s^2 \simeq \frac{(nZ)' + 2Z^2/3}{Z + x + 3/2}, \qquad (31)$$

where $x = m/T$. Equations (30) and (31) clearly show that HSI leads to superluminal sound velocities $c_s > 1$ at sufficiently high densities where Z is large (for further discussion, see Ref. [7]). This is especially evident in the EVM where $(nZ)' = Z^2$. According to Eq. (31), in this case c_s^2 is proportional to Z at large Z.

In Fig. 2 we compare the sound velocities calculated by using the parametrizations (3) and (4) for two typical values of

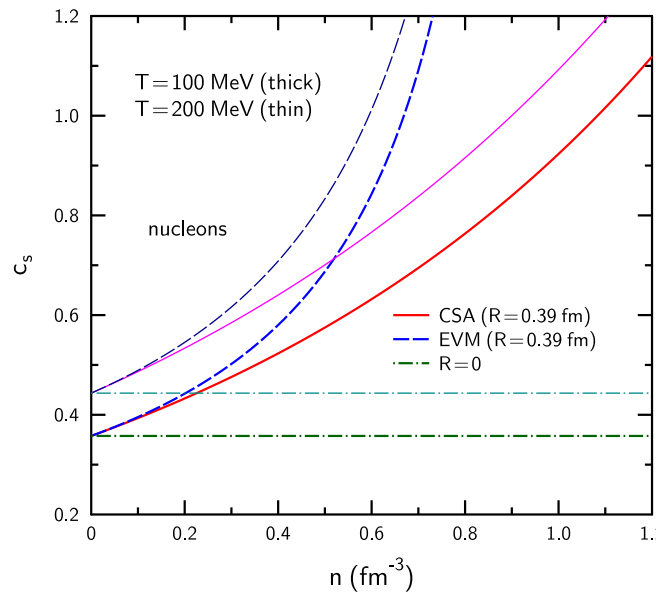

FIG. 2. (Color online) Sound velocity of nucleon gas as a function of density for two values of temperature $T = 100$ (thick lines) and 200 (thin lines) MeV. The solid and dashed curves are calculated by using compressibility functions proposed in the CSA and EVM. The dash-dotted lines are obtained in the limit of point-like nucleons ($R = 0$).

[6]This result is rather obvious. It is clear that the energy per particle, ε/n, for a one-component system with classical hard-sphere particles should depend only on temperature, at least for densities below the liquid-solid transition. Therefore, increasing the density at fixed T does not change ε/n.

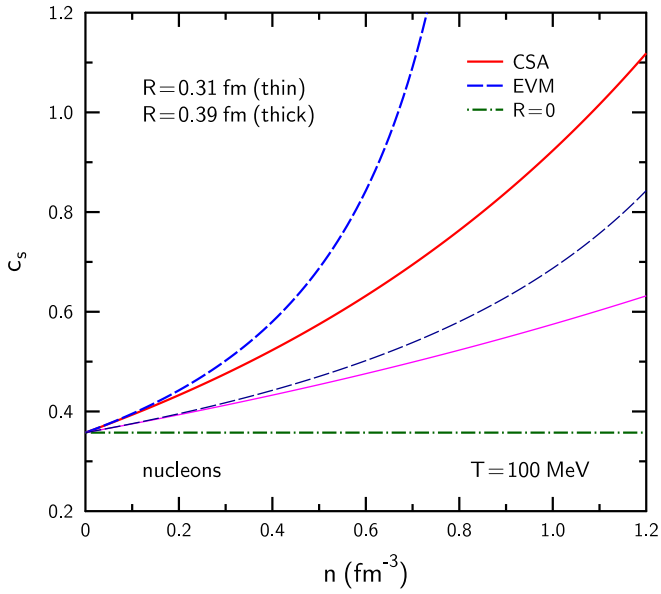

FIG. 3. (Color online) Sound velocity of nucleonic matter as a function of density for different values of parameter R. The dashed and solid curves are calculated, respectively, in the EVM and CSA. The dash-dotted line corresponds to point-like nucleons.

temperature. We have chosen the nucleon radius $R = 0.39$ fm which corresponds to the excluded volume $b = 1$ fm^3, used previously in Ref. [7]. Again one can see that the CSA predicts a much softer EoS (i.e., smaller c_s) than the EVM. Our calculations show that, at realistic temperatures $T \lesssim 200$ MeV, the sound velocity in the CSA remains below unity up to rather large densities $n \simeq 0.9$ fm^{-3}. On the other hand, superluminal sound velocities appear in the EVM at much smaller n. According to Fig. 2, deviations from the ideal-gas limit $R \to 0$ become significant already at subnuclear densities $n \sim 0.1$ fm^{-3}.

Figure 3 demonstrates that the sound velocity is very sensitive to the choice of the particle size R. Note that a 20% reduction of R, from 0.39 to 0.31 fm, corresponds to the twofold decrease of the excluded volume b. It is seen that the difference between CSA and EVM is smaller for lower R. Figure 4 shows the results for the baryon chemical potential as a function of nucleon density and pressure. One can see that at $n \gtrsim 0.4$ fm^{-3} the CSA indeed predicts significantly smaller values of μ as compared to the EVM. On the other hand, at given μ the pressure in the CSA is noticeably larger than in the EVM. This makes the nucleon phase more stable at high densities as compared to the EVM.

E. Pion matter

Let us consider now thermodynamic properties of matter composed of finite-size "thermal" pions with the vacuum mass $m_\pi = 140$ MeV and the statistical weight $g_\pi = 3$. As before, we assume the hard-sphere interaction of particles and perform all calculations in the Boltzmann approximation. To emphasize specific features of the pion system we introduce the subscript "π." Using Eqs. (1), (22), one can write the following equations for pressure and chemical potential of pions

$$P_\pi = T n_\pi Z(n_\pi), \quad \mu_\pi = T\left[\ln\frac{n_\pi}{\phi_\pi(T)} + \psi(n_\pi)\right], \qquad (32)$$

where ϕ_π and ψ are defined in Eqs. (6) and (21) (with $m = m_\pi, g = g_\pi$).

At fixed temperature one can find equilibrium values of density $n_\pi = n_\pi(T)$ and other thermodynamic functions from the condition of chemical equilibrium $\mu_\pi = 0$. Then we obtain the following implicit equation for density of pions:

$$n_\pi = \phi_\pi(T) e^{-\psi(n_\pi)}. \qquad (33)$$

As one can see from Eq. (33), finite-size effects suppress the pion density as compared to the ideal-gas limit $\psi \to 0$. This is illustrated in Fig. 5 where we compare the results of the

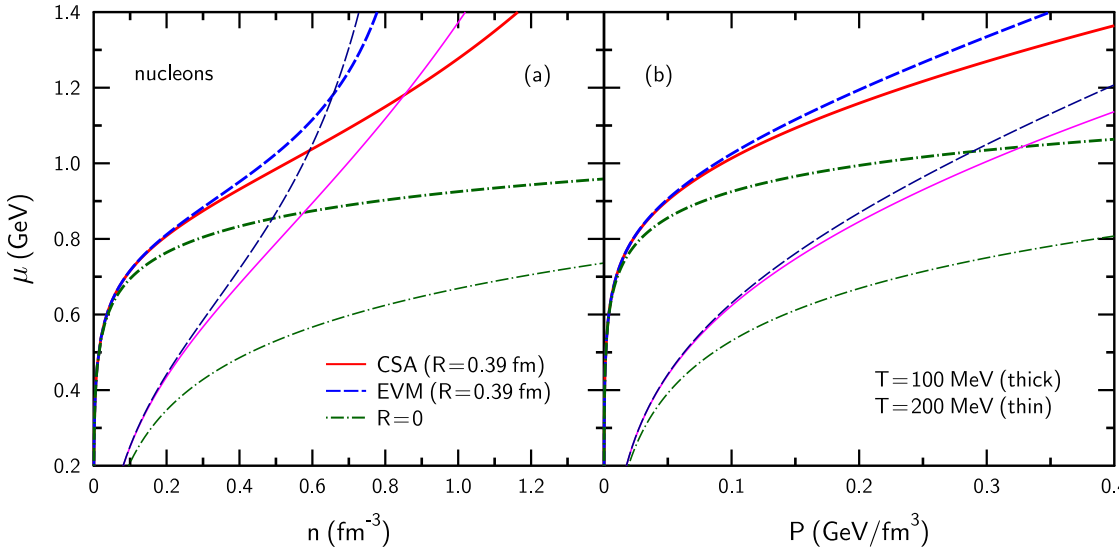

FIG. 4. (Color online) Chemical potential of nucleon gas as a function of (a) density and (b) pressure calculated in the CSA (solid lines) and EVM (dashed lines) at temperatures of 100 and 200 MeV. The dash-dotted lines correspond to point-like nucleons.

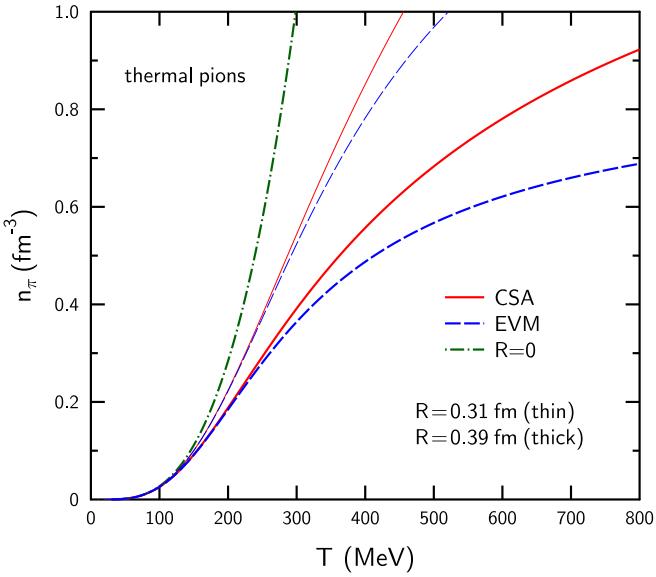

FIG. 5. (Color online) Equilibrium density of pions as a function of temperature for different values of parameter R. The dashed and solid curves are obtained, respectively, in the EVM and CSA. The dash-dotted line corresponds to ideal gas of point-like pions.

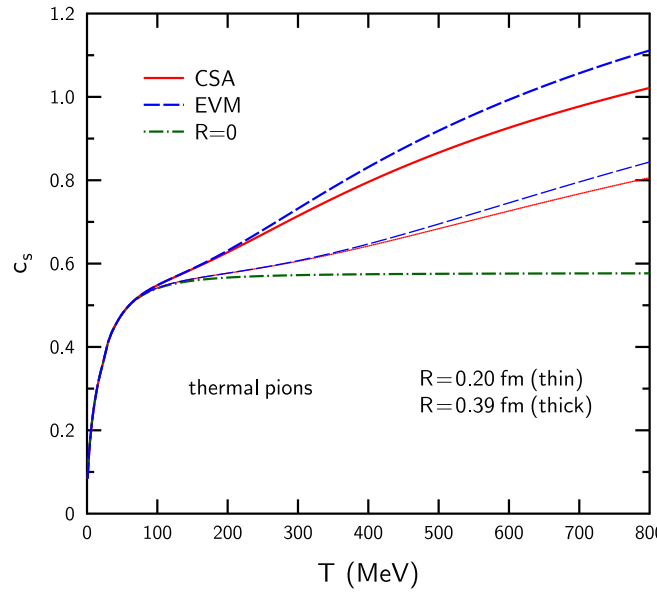

FIG. 6. (Color online) Sound velocity of pion gas as a function of temperature for different values of parameter R. The dashed and solid curves are calculated, respectively, in the EVM and CSA. The dash-dotted line corresponds to point-like pions.

EVM and CSA, for several values of the hadronic radius R. One can see noticeable deviations from the ideal gas already at $T \simeq 150$ MeV, but a significant difference between the CSA and EVM calculations appears only at unrealistically high temperatures $T \gtrsim 400$ MeV. Such behavior follows from a relatively slow increase of pion packing ratio with temperature. Note that short-range repulsive interactions of pions also suppress possible Bose-enhancement effects at high temperatures (see Sec. III F).

One can easily calculate the entropy density of interacting pion gas. In the case $\mu_\pi = 0$, using the thermodynamic relation $s_\pi = dP_\pi/dT$, one has

$$s_\pi = T\frac{dn_\pi}{dT}(n_\pi Z)' + n_\pi Z = n_\pi(Z + \xi_\pi - 1), \qquad (34)$$

where prime denotes the derivative with respect to the density n_π and ξ_π is defined in Eq. (11). In the second equality we use the relation

$$T\frac{dn_\pi}{dT} = \frac{n_\pi(\xi_\pi - 1)}{1 + n_\pi\psi'} = \frac{n_\pi(\xi_\pi - 1)}{(n_\pi Z)'}, \qquad (35)$$

which follows from Eq. (33) after taking the derivative with respect to T. According to Eqs. (34) and (18) the entropy per pion s_π/n_π equals approximately $Z + 3$ at $T \gg m_\pi$. This value exceeds the corresponding ratio for massless point-like pions ($Z = 1$).

Equation (34) leads to the following formula for the energy density $\varepsilon_\pi = Ts_\pi - P_\pi$:

$$\varepsilon_\pi = n_\pi T(\xi_\pi - 1). \qquad (36)$$

From this result one can see that, at a given temperature, the energy per particle is the same as in the ideal pion gas. Using Eqs. (35), (36), and (12) we get the equation for the heat capacity per pion $\widetilde{C}_\pi = n_\pi^{-1} d\varepsilon_\pi/dT$:

$$\widetilde{C}_\pi = x_\pi^2 + 3\xi_\pi + (\xi_\pi - 1)^2\left[\frac{1}{(n_\pi Z)'} - 1\right], \qquad (37)$$

where $x_\pi = m_\pi/T$.

Finally we obtain the following formula for the sound velocity squared:

$$c_s^2 = \frac{dP_\pi}{d\varepsilon_\pi} = \frac{s_\pi}{n_\pi\widetilde{C}_\pi} = \frac{Z + \xi_\pi - 1}{\widetilde{C}_\pi}. \qquad (38)$$

In the ideal-gas limit $Z \to 1$ one gets $c_s = (3 + x_\pi^2/\xi_\pi)^{-1/2} = (3 + x_\pi K_2/K_3)^{-1/2}$. By using Eq. (18) we arrive at the approximate relation

$$c_s^2 \simeq \frac{1}{3}(Z + n_\pi Z')\left(1 + \frac{n_\pi Z'}{Z + 3}\right)^{-1} \qquad (39)$$

in the ultrarelativistic case $x_\pi \ll 1$. Figure 6 shows the results of c_s calculations with the parameters $R = 0.20$ and 0.39 fm. One can see that at $T \gtrsim 200$ MeV the obtained sound velocities noticeably exceed the asymptotic ideal-gas value $c_s = 1/\sqrt{3}$. The calculations show that these velocities become superluminal only at unrealistically high temperatures at which hadrons should melt [19,20].

III. HADRONIC MIXTURES

A. General remarks

Let us consider now a multicomponent hadronic matter composed of particles of different kinds $i = 1,2,\ldots$. Most detailed information about the EoS of this matter can be obtained if one knows its pressure $P = P(T,n_1,n_2,\ldots)$ as a function of temperature T and partial densities $n_i = N_i/V$. As before, we neglect the quantum effects and assume that

particles interact via HSI. In this case one can write down [3] the first two terms of the virial expansion of pressure in powers of n_i:

$$\frac{P}{nT} = 1 + \sum_{i,j} b_{ij} x_i x_j + \cdots . \tag{40}$$

Here $n = \sum_i n_i$ is the total density, $x_i = n_i/n$, and coefficients $b_{ij} = \frac{2\pi n}{3}(R_i + R_j)^3$, where R_i is the radius of the ith species. If particle radii are the same ($R_i = R$ for all i) the second term in the r.h.s. equals 4η where $\eta = 4\pi R^3 n/3$. In this limit most of the results for one-and multicomponent systems will be formally the same. In particular, one may use Eq. (1) and the formulas for thermodynamic functions from Sec. II D by identifying the variable n with the total density of all species.

It is possible to calculate the shift of the free-energy density, Δf, for any multicomponent system if one knows its pressure as a function of temperature and partial densities. Below we use the method suggested in Ref. [21]. Using the thermodynamic relation $dF = -PdV$ for the change of total free energy F in the isothermal process, one can write down the equation connecting the shifts of F and P:

$$\Delta F = \int_V^\infty dV_* \Delta P\left(T, \frac{N_1}{V_*}, \frac{N_2}{V_*}, \dots\right). \tag{41}$$

The r.h.s. of this equation is equal to the work done by particle interactions during the isothermal compression of matter from an asymptotically large volume to $V_* = V$. Introducing the variable $\alpha = V/V_*$ one obtains the expression for $\Delta f = \Delta F/V$:

$$\Delta f = \int_0^1 \frac{d\alpha}{\alpha^2} \Delta P(T, \alpha n_1, \alpha n_2, \dots). \tag{42}$$

For a one-component matter with HSI, substituting $\Delta P = nT(Z-1)$, we return to the formulas obtained in Sec. II D.

It is easy to derive exact results for mixtures where one of the components consists of point-like particles. Namely, let us consider a two-component system where the ratio of particle radii R_2/R_1 is small. In the limit $R_2 \to 0$ one can regard the component $i = 2$ as an ideal gas but in the reduced "free" volume $\widetilde{V} = V - N_1 v_1 = V(1-\eta_1)$. Here v_1 and η_1 are, respectively, the proper volume and the packing fraction of particles $i = 1$. The partial pressure of the first component may be written analogously to Eq. (1). This leads to the following equation for pressure of a two-component mixture with $R_2/R_1 \ll 1$ [3]:

$$P(T, n_1, n_2) = n_1 T Z(n_1) + \frac{n_2 T}{1-\eta_1}. \tag{43}$$

The last term is the partial pressure of the second component $P_2 = \widetilde{n}_2 T$. Here $\widetilde{n}_2 = N_2/\widetilde{V}$ is the "local" density of particles $i = 2$ which is larger than the "average" density $n_2 = N_2/V$. Using Eq. (43) one can easily prove the validity of the virial theorem (40) in the limit $n_1, n_2 \to 0$. In fact, instead of particles $i = 1$ we can consider an arbitrary multicomponent mixture composed of hadrons with the same radii. In this case n_1 equals the total density of such a mixture.

B. $N + \Delta$ matter

In this section we consider the EoS of a chemically equilibrated binary mixture of baryons: nucleons (N) and the lightest Δ resonances ($m_\Delta = 1232$ MeV, $g_\Delta = 16$). This system is characterized by two canonical variables: temperature and the baryon density $n_B = n_N + n_\Delta$. We assume that all baryons have the same radii, i.e., $R_N = R_\Delta = R$. In this case HSI does not distinguish N and Δ, therefore, the hadronic pressure can be written as $P = n_B T Z(n_B)$. The same arguments as used in deriving Eq. (22) lead to the equation for chemical potential of the ith species ($i = N, \Delta$):

$$\mu_i = T\left[\ln \frac{n_i}{\phi_i(T)} + \psi(n_B)\right]. \tag{44}$$

Here ϕ_i is defined in Eq. (6) with the replacement $m \to m_i, g \to g_i$.

From the condition of chemical equilibrium $\mu_N = \mu_\Delta = \mu_B$ we get the expressions

$$\mu_B = T\left[\ln \frac{n_B}{\phi_N + \phi_\Delta} + \psi(n_B)\right], \tag{45}$$

$$n_i = n_B w_i(T), \quad w_\Delta = 1 - w_N = \frac{\phi_\Delta}{\phi_N + \phi_\Delta}. \tag{46}$$

The relative fractions of ith baryons, w_i, depend on temperature only and coincide with corresponding values for the ideal gas of $N + \Delta$ baryons [22].

Using Eq. (45) one obtains the formula for the free-energy density,

$$f = \mu_B n_B - P = n_B T \left\{\ln \frac{n_B}{\phi_N + \phi_\Delta} - 1 + \int_0^{n_B} \frac{dn_1}{n_1}[Z(n_1) - 1]\right\}. \tag{47}$$

This leads to the following equations for the energy density and isochoric heat capacity of the $N + \Delta$ mixture:

$$\varepsilon = f - T\left(\frac{\partial f}{\partial T}\right)_{n_B} = n_B T \langle \xi - 1 \rangle, \tag{48}$$

$$C_V = \left(\frac{\partial \varepsilon}{\partial T}\right)_{n_B} = n_B[\langle x^2 + 3\xi \rangle - \langle \xi - 1 \rangle^2] \equiv n_B \widetilde{C}(T). \tag{49}$$

Angular brackets in Eqs. (48) and (49) denote averaging over the concentrations of N and Δ particles. Namely, we define $\langle A \rangle = \sum_{i=N,\Delta} A_i w_i$ where w_i is introduced in Eq. (46) and A_i is any quantity characterizing the ith component. In particular, $\langle \xi \rangle = \xi_N w_N + \xi_\Delta w_\Delta$ where ξ_i is defined in Eq. (11). As one can see from Eqs. (48) and (49), the energy and heat capacity densities are the same as in the ideal gas of $N + \Delta$ particles [22].

Figure 7(a) shows the temperature dependence of the total energy per baryon E/B as well as the partial contributions to this quantity, $E_i/B = T(\xi_i - 1)w_i$ ($i = N, \Delta$). Note that all quantities considered in Figs. 7(a) and 7(b) are functions of temperature only and do not depend on the baryon density (in the Boltzmann approximation). At fixed baryon charge $B = N_N + N_\Delta$ the equilibrium number of Δs increases

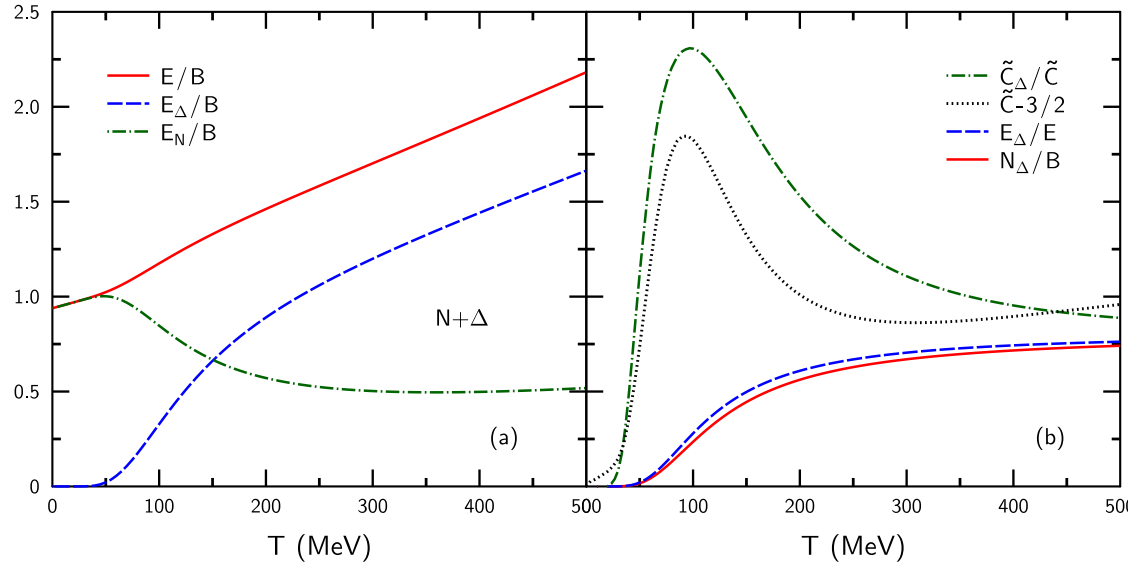

FIG. 7. (Color online) (a) The average energy per baryon of $N+\Delta$ matter E/B and partial contributions of nucleons and Δs as functions of temperature (all energies are given in GeV). (b) The dashed, solid, and dash-dotted curves show, respectively, relative contributions of resonances to energy, baryon charge, and heat capacity. The dotted line shows temperature dependence of the total heat capacity per baryon minus 3/2.

with temperature. One can see that excitation of resonances becomes important at $T \gtrsim 50$ MeV. It is interesting to note that the nucleon part of energy, E_N, drops with temperature[7] in the interval of T approximately between 50 and 350 MeV. Introducing the partial components $\widetilde{C}_i = B^{-1} dE_i/dT$ of the total heat capacity $\widetilde{C}$ we conclude that the nucleon contribution, $\widetilde{C}_N = \widetilde{C} - \widetilde{C}_\Delta$, is negative in the above-mentioned interval of T. One can see from Fig. 7(b) that $\widetilde{C}_\Delta > \widetilde{C}$ in this region.

Now we calculate the sound velocity of equilibrium hadronic matter by using the general formula [23]

$$c_s^2 = \frac{1}{\varepsilon + P}\left[n_B \left(\frac{\partial P}{\partial n_B}\right)_T + \frac{T}{C_V}\left(\frac{\partial P}{\partial T}\right)_{n_B}^2 \right]. \qquad (50)$$

Note that calculating c_s from Eq. (50) does not require an explicit form of the Poisson adiabat: one should know only P and ε as well as their partial derivatives with respect to T and n_B. We would like to stress that Eq. (50) is applicable for any form of short-range interaction, for any number of hadronic species (including antibaryons and strange particles) and can be used even in the case of quantum statistics.

For a given EoS, one can use Eq. (50) to check constraints imposed by the causality condition $c_s \le 1$. For example, for the polytropic EoS $P = \alpha n_B^\gamma$ at zero temperature, Eq. (50) predicts that

$$c_s^2 = P'(n_B)\left[\int_0^{n_B} \frac{dn}{n} P'(n)\right]^{-1} = \gamma - 1.$$

Therefore, in this case the parameter γ should satisfy the condition[8] $1 \le \gamma \le 2$.

One can calculate the sound velocity of the $N+\Delta$ mixture using Eq. (50) and formulas for P, ε, C_V derived in this section. We arrive at the following result:

$$c_s^2 = \frac{(n_B Z)' + Z^2 \widetilde{C}^{-1}}{\langle \xi \rangle + Z - 1}, \qquad (51)$$

where prime denotes the derivative with respect to n_B. Note that this formula can also be obtained from Eq. (30) if one replaces n, ξ by $n_B, \langle \xi \rangle$ and uses, instead of Eq. (12), the expression (49) for $\widetilde{C}$.

Figure 8 shows the results of c_s calculation in the EVM and CSA. We choose the hadron hard-core radius $R = 0.39$ fm. Again one can see that the CSA predicts smaller sound velocities than the EVM. As compared to the EVM, the sound velocity in the CSA increases with n_B much slower, but the temperature dependence is rather similar. In Fig. 9 we compare the sound velocities of the nucleonic and $N+\Delta$ matter. Both calculations are made in the CSA. The ideal gas results are obtained by taking the limit $n_B \to 0$. One can see that inclusion of resonances leads to a noticeable reduction of sound velocities at $T \gtrsim 50$ MeV. For realistic temperatures $T \lesssim 200$ MeV, superluminal values $c_s > 1$ appear only at baryon densities $n_B \gtrsim 1$ fm^{-3}.

The $N+\Delta$ mixture considered so far cannot be regarded as a realistic system at high temperatures. In this case mesons will be copiously produced due to inelastic collisions of baryons and decays of resonances. To take these processes into account, in Secs. III C and III D we investigate the EoS of a three-component $\pi + N + \Delta$ mixture. In this study we again assume

[7]This occurs because the growth of the nucleon single-particle energy, $E_N/N_N = T(\xi_N - 1)$, with raising T is compensated by a stronger decrease of the number of nucleons $N_N(T) = w_N(T)B$.

[8]The causal limit for the polytropic EoS was first considered in Ref. [24].

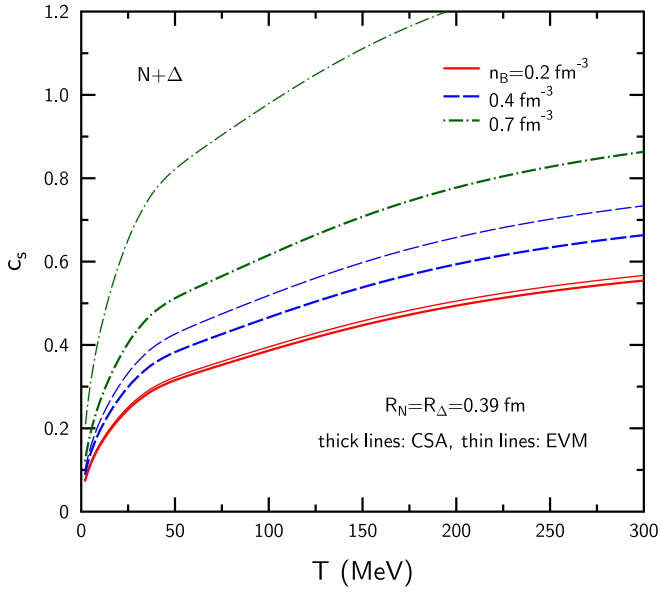

FIG. 8. (Color online) Sound velocity of $N+\Delta$ matter as a function of temperature for several values of baryon density n_B. Thick and thin curves give the results of CSA and EVM, respectively.

that hadrons interact via HSI and neglect possible differences in baryonic radii, i.e., we take $R_N = R_\Delta = R$. To estimate the sensitivity to the pion size, we consider two limiting cases. First, we assume equal radii for all species, i.e., we choose $R_\pi = R$, and then we investigate the $\pi + N + \Delta$ mixture with point-like pions ($R_\pi = 0$).

C. $\pi + N + \Delta$ matter (same size of hadrons)

In this section we consider the $\pi + N + \Delta$ mixture assuming equal sizes of all hadrons. In this case one can find shifts of thermodynamic functions in the same way as in Sec. II C for a one-component system. The only difference is that instead of particle density n one should substitute the total density of hadrons $n_\pi + n_B$. As a result, we obtain the relations

$$P = nTZ(n), \quad n = n_\pi + n_B, \tag{52}$$

$$\mu_i = T\left[\ln\frac{n_i}{\phi_i(T)} + \psi(n)\right], \tag{53}$$

for pressure and chemical potentials of particle species $i = \pi, N, \Delta$. Using the conditions of chemical equilibrium $\mu_\pi = 0$, $\mu_N = \mu_\Delta = \mu_B$, one gets the equations for equilibrium pion density,

$$n_\pi = \phi_\pi(T)e^{-\psi(n_\pi+n_B)}, \tag{54}$$

and for baryon chemical potential,

$$\mu_B = T\left[\ln\frac{n_B}{\phi_N+\phi_\Delta} + \psi(n_\pi+n_B)\right]. \tag{55}$$

Solving Eq. (54) with respect to n_π and substituting the result into Eq. (52) gives the equilibrium pressure $P = P(T, n_B)$ of the considered mixture. Similarly to Sec. III B, one can show that equilibrium fractions n_N/n_B and n_Δ/n_B are the same as in the ideal $N+\Delta$ gas [see Eq. (46)]. According to Eq. (54), interaction with baryons leads to suppression of pion density as compared to pure pion gas ($n_B = 0$). This is demonstrated in Fig. 10 (see the solid and short-dashed curves).

Calculating further the free-energy density $f = \mu_B n_B - P$ and using Eqs. (5), (54), and (55) lead to the following

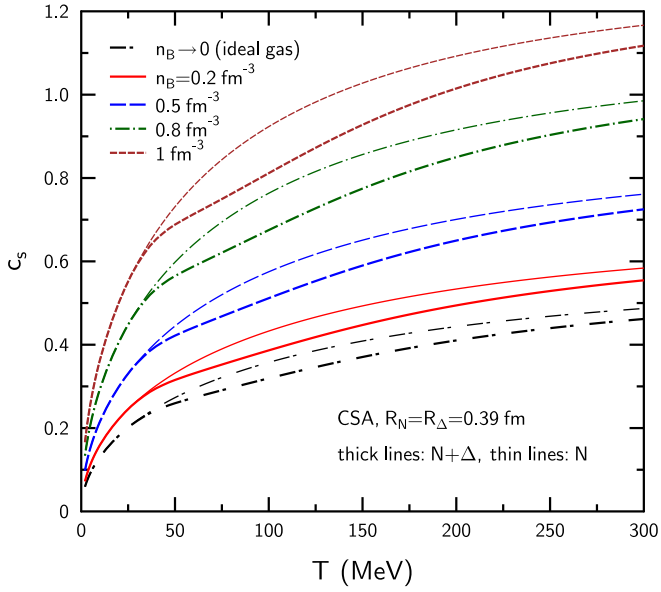

FIG. 9. (Color online) Sound velocities of baryon matter as functions of temperature for different values of baryon density n_B. Thin and thick lines correspond, respectively, to the nucleon matter and to the $N+\Delta$ mixture. All calculations are made in the CSA.

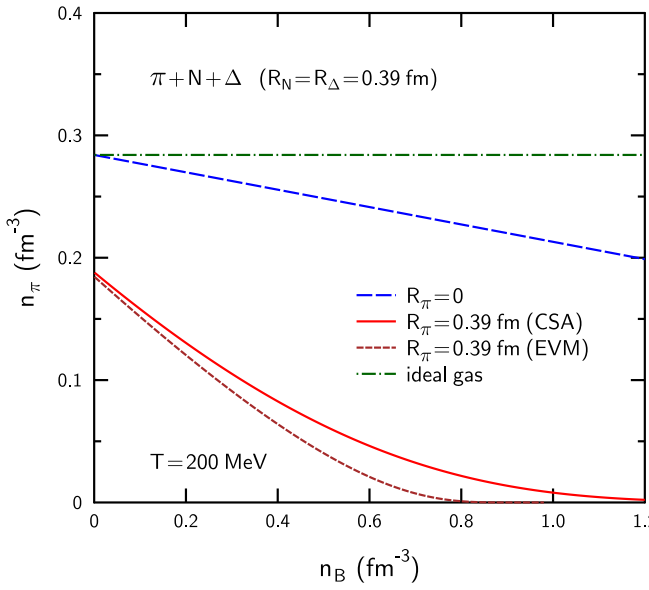

FIG. 10. (Color online) Equilibrium pion density in $\pi + N + \Delta$ mixture as a function of baryon density for $T = 200$ MeV. The solid and short-dashed curves are calculated within CSA and EVM assuming equal sizes of hadrons. The long-dashed line is obtained in the limit of point-like pions. The dashed-dotted curve corresponds to the ideal gas.

equations for the energy density and heat capacity:

$$\varepsilon = T[n_B\langle\xi - 1\rangle + n_\pi(\xi_\pi - 1)], \tag{56}$$

$$C_V = n_B[\langle x^2 + 3\xi\rangle - \langle\xi - 1\rangle^2] + n_\pi\big[x_\pi^2 + 3\xi_\pi - (\xi_\pi - 1)^2(1 - \chi)\big], \tag{57}$$

where

$$\chi = 1 + \left(\frac{\partial n_\pi}{\partial n_B}\right)_T = [1 + n_\pi\psi'(n)]^{-1}$$

(here and below prime denotes the derivative with respect to n) . Note that Eq. (56) formally corresponds to the ideal $\pi + N + \Delta$ gas, but with reduced pion density $n_\pi < n_\pi^{\rm id} = \phi_\pi(T)$.

Using Eq. (50), one can calculate the sound velocity of the considered matter. We use the following expressions for the derivatives of pressure:

$$\left(\frac{\partial P}{\partial n_B}\right)_T = T\chi(nZ)', \qquad \left(\frac{\partial P}{\partial T}\right)_{n_B} = nZ + \chi(nZ)'n_\pi(\xi_\pi - 1). \tag{58}$$

The results of c_s calculation are shown by the solid lines in Fig. 11 for two values of temperature. The local minima of c_s at $n_B \sim 0.2$ fm^{-3} appear due to a nonmonotonic behavior of the total density $n_\pi + n_B$ as a function of n_B. Again one can see that compared to EVM, the region of superluminal sound velocities in CSA is shifted to higher baryon densities.

D. $\pi + N + \Delta$ mixture with point-like pions

Finally, we consider the limiting case of point-like pions ($R_\pi = 0$). In accordance with Eq. (43), in this case one can represent pressure of the $\pi + N + \Delta$ system as

$$P = P(T, n_\pi, n_N, n_\Delta) = T\left[\frac{n_\pi}{1 - \eta} + n_B Z(n_B)\right], \tag{59}$$

where $\eta = v n_B$ (v is the proper volume of a baryon) and $n_B = n_N + n_\Delta$. The compressibility factor Z describes the contribution of baryon interactions. Below we use the parametrizations of Z from Eqs. (3) and (4). Substituting $\Delta P = P - (n_\pi + n_B)T$ into Eq. (42), one can write the shift of free-energy density as follows:

$$\Delta f = f - T\sum_{i=\pi,N,\Delta} n_i\left[\ln\frac{n_i}{\phi_i(T)} - 1\right] = T\left\{n_\pi \ln(1 - \eta)^{-1} + n_B\int_0^{n_B}\frac{dn_1}{n_1}[Z(n_1) - 1]\right\}. \tag{60}$$

Using further the conditions of chemical equilibrium

$$\mu_\pi = \frac{\partial f}{\partial n_\pi} = 0, \quad \mu_B = \frac{\partial f}{\partial n_N} = \frac{\partial f}{\partial n_\Delta}, \tag{61}$$

we get the equations for equilibrium densities $n_i (i = \pi, N, \Delta)$ as functions of T and n_B. In this way one obtains the same formulas for n_N and n_Δ as for $N + \Delta$ matter [see Eq. (46)]. From Eq. (61) we get the relation

$$\mu_B = T\left[\ln\frac{n_B}{\phi_N + \phi_\Delta} + \psi(n_B) + v\phi_\pi\right]. \tag{62}$$

One can see from Eqs. (45) and (62) that inclusion of point-like pions leads to the additional term of the baryon chemical potential, $\delta\mu_B = T\phi_\pi v$, as compared to the $N + \Delta$ system. This contribution has a clear physical meaning. Indeed, to add one baryon to the system of point-like pions, one should create a cavity of volume v. At fixed temperature this requires the additional energy (work) $\delta E = P_\pi v$, where $P_\pi = T\phi_\pi$ is the partial pressure of pions (see below). Therefore, the baryon

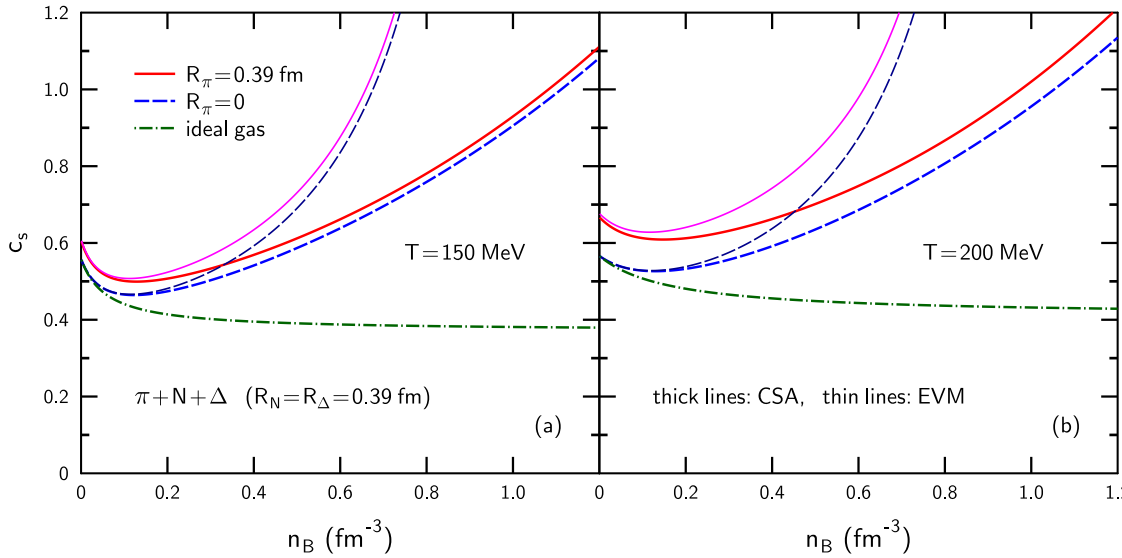

FIG. 11. (Color online) Sound velocity of $\pi + N + \Delta$ matter as a function of baryon density for (a) $T = 150$ MeV and (b) 200 MeV. Thick and thin curves give, respectively, the results of CSA and EVM. The solid lines correspond to the case of equal sizes of baryons and pions. The dashed lines show the results in the limit of point-like pions. The dash-dotted curves correspond to the ideal gas.

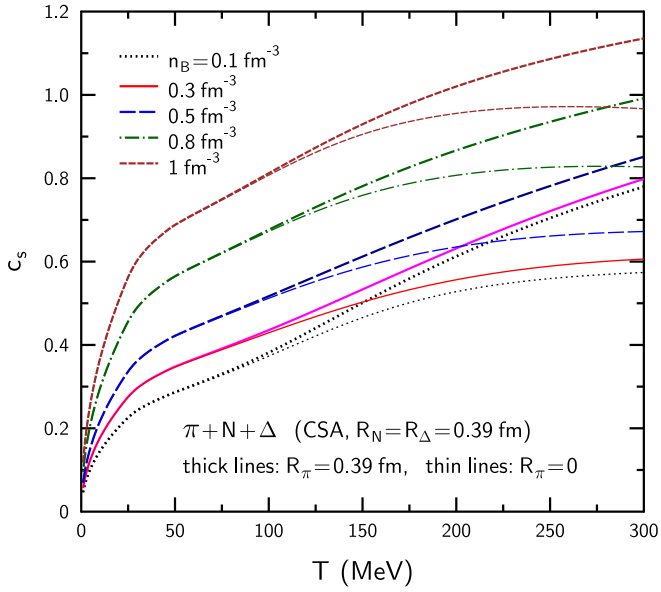

FIG. 12. (Color online) Sound velocity of $\pi + N + \Delta$ matter as a function of temperature for different values of baryon density n_B. Thick and thin lines are calculated within the CSA assuming, respectively, the pion radii $R_\pi = 0.39$ fm and $R_\pi = 0$.

chemical potential should be shifted by the value $\delta\mu_B = P_\pi v$. Note that this shift may be significant even at small n_B.

Equilibrium values of pion density and pressure can be written as

$$n_\pi = \phi_\pi(T)(1-\eta), \quad P = T[\phi_\pi(T) + n_B Z(n_B)]. \tag{63}$$

The last factor in the first equality describes the reduction of volume, available to pions. A linear decrease of n_π as a function of n_B is clearly seen in Fig. 10. One can also obtain the explicit formulas for ε and C_V. They are given by Eqs. (56) and (57) after substituting $\chi = 1$.

Using further Eq. (50) we get the equation for sound velocity squared,

$$c_s^2 = \frac{n_B(n_B Z)' + C_V^{-1}(\xi_\pi\phi_\pi + n_B Z)^2}{n_B[\langle\xi\rangle + Z - 1] + \phi_\pi[\xi_\pi(1-\eta) + \eta]}. \tag{64}$$

At small T, when $\phi_\pi \ll 1$, one obtains Eq. (51) for the sound velocity of the $N + \Delta$ mixture. In Figs. 11 and 12 we compare the results of c_s calculations for $R_\pi = 0.39$ fm and $R_\pi = 0$. As expected, at fixed T and n_B the sound velocity increases with R_π. A realistic value for R_π is somewhere between the two considered cases. Based on the results presented in Fig. 12 we conclude that the EoS for the $\pi + N + \Delta$ mixture remains causal up to the baryonic densities where the deconfinement phase transition is expected.

E. Extended set of hadrons: baryons, antibaryons, and mesons

In this section we consider a multicomponent hadronic system, which includes baryons ($i = N, \Delta, \Lambda, \ldots$), antibaryons ($i = \overline{N}, \overline{\Delta}, \overline{\Lambda}, \ldots$), and mesons ($i = \pi, K, \overline{K}, \ldots$). We take into account all observed hadrons with masses below 2 GeV.[9] As before, the isospin and Coulomb effects are neglected, and hadronic resonances are treated in the zero-width approximation. Below we consider the simplest case when all hadrons have the same hard-core radii ($R_i = R$).

At given temperature and fixed chemical potentials $\{\mu_i\}$ one can find partial densities of different hadronic species $\{n_i\}$ by generalizing the procedure described in Sec. III C. We obtain the relations

$$n_i = n_i^{\rm id}(T, \mu_i) e^{-\psi(n_T)}, \tag{65}$$

where the first factor is the partial density of the ideal gas of ith hadrons:

$$n_i^{\rm id}(T, \mu_i) = \phi_i(T) e^{\mu_i/T}. \tag{66}$$

The quantity $\psi(n_T)$ is defined by Eq. (21) with replacing n by the total density of all hadronic species $n_T = \sum_i n_i$. By taking sum over all i we get from Eq. (65) an implicit equation for n_T:

$$n_T = e^{-\psi(n_T)} n_T^{\rm id}, \tag{67}$$

where $n_T^{\rm id} = \sum_i n_i^{\rm id}$. At given T and $\{\mu_i\}$ one can calculate n_T and the hadron abundances n_i from Eqs. (65)–(67).

Generalizing Eqs. (52) and (56) for the case of a multicomponent hadronic gas leads to the following expressions for pressure and energy density:

$$P = T n_T Z(n_T), \tag{68}$$

$$\varepsilon = T \sum_i n_i [\xi_i(T) - 1]. \tag{69}$$

The net-baryon and net-strangeness densities of hadronic matter are defined as follows:

$$n_B = \sum_i B_i n_i, \quad n_S = \sum_i S_i n_i, \tag{70}$$

where $B_i = 0, \pm 1$ and $S_i = 0, \pm 1, \pm 2, \pm 3$ are, respectively, the baryon charge and the strangeness number of hadrons. At given chemical potentials these densities are reduced by the factor $\exp(-\psi)$ as compared to the ideal gas.

The condition of chemical equilibrium with respect to strong interactions leads to the general expression for chemical potentials of different species:

$$\mu_i = B_i \mu_B + S_i \mu_S, \tag{71}$$

where μ_B and μ_S are, respectively, the baryon and strange chemical potentials. Below we assume that total strangeness of the hadronic system is equal to zero.[10] In this case one can calculate μ_S from the condition of strangeness neutrality

$$n_S(T, \mu_B, \mu_S) = 0. \tag{72}$$

By using Eqs. (65)–(72) one may find all thermodynamic quantities of nonstrange hadronic matter as functions of T

[9] We include the same set of hadrons as in Ref. [7].

[10] Note that hadronic matter with nonzero net strangeness can be formed in compact stars and at intermediate stages of heavy-ion collisions [7].

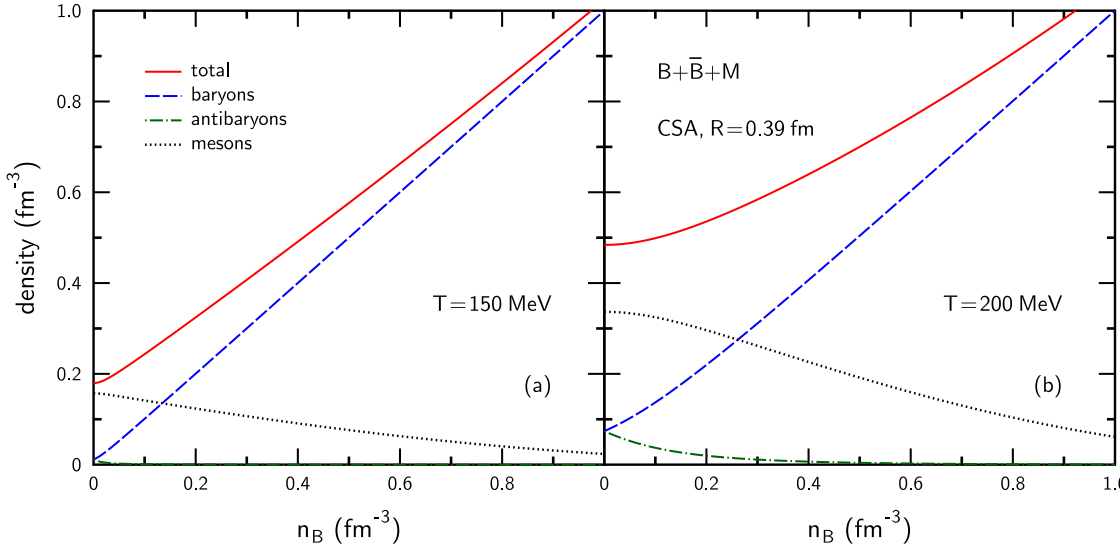

FIG. 13. (Color online) Total density of hadronic matter as well as its contributions from baryons, antibaryons, and mesons as functions of the net baryon density n_B for (a) $T = 150$ MeV and (b) 200 MeV. All calculations are made in the CSA assuming the hadronic radius $R = 0.39$ fm.

and n_B. Then Eq. (50) can be used to determine the sound velocity c_s.

In Figs. 13 and 14 we present the results of the CSA calculation for $R = 0.39$ fm. According to Fig. 13, relative abundances of antibaryons rapidly drop with raising n_B. Even at small n_B they do not exceed 6% and 15% at temperatures 150 and 200 MeV, respectively. Our calculations show that at $n_B \to 0$ the partial densities of different hadrons are reduced as compared to the ideal gas by about 30% and 70% at $T = 150$ and 200 MeV. One can see from Fig. 13 that, at fixed temperature, baryons become more abundant than mesons at large enough n_B. Our calculations show that at $T = 150$ MeV this occurs at $n_B > 0.13$ fm^{-3} which corresponds to $\mu_B > 440$ MeV. It is interesting that a similar conclusion has been drawn [25] from the thermal fit of hadron ratios observed in heavy-ion collisions at AGS and SPS bombarding energies. It has been shown that the transition from a meson-dominated to a baryon-dominated matter occurs at center-of-mass energy $\sqrt{s_{NN}} \simeq 8.2$ GeV for which the freeze-out parameters are $T \simeq 140$ MeV, $\mu_B \simeq 410$ MeV. As one can see from Fig. 13(a), the abundance of antibaryons is negligible at these conditions.

Figure 14 represents the sound velocity as a function of n_B for the same values of temperature as in Fig. 13. One can see that c_s values are slightly reduced as compared with the

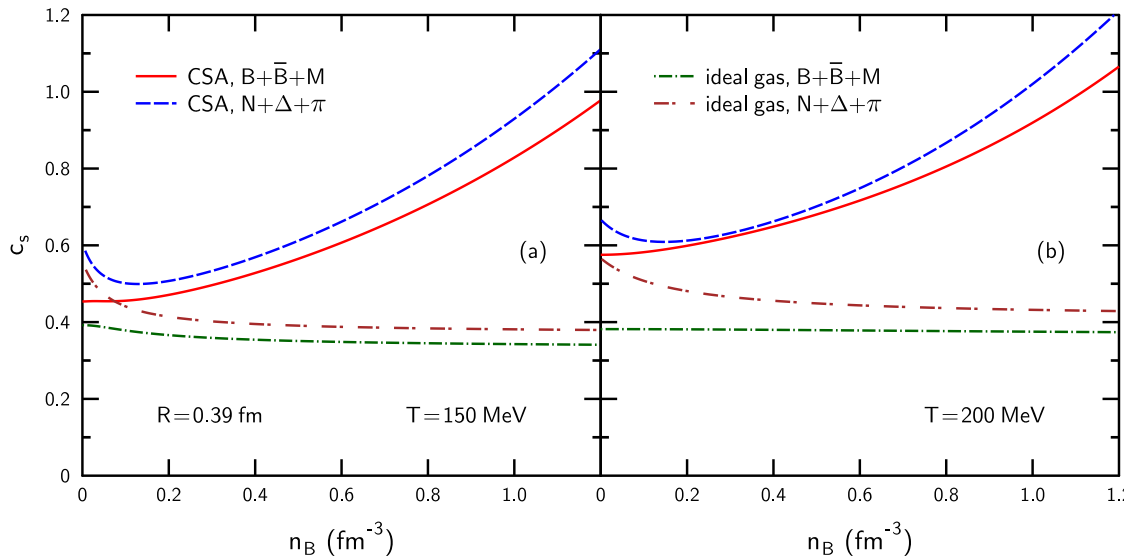

FIG. 14. (Color online) Sound velocity of hadronic matter as a function of net baryon density for (a) $T = 150$ MeV and (b) 200 MeV. The solid and dashed lines correspond, respectively to the (anti)baryon-meson and $N + \Delta + \pi$ matter. The calculations are made in the CSA assuming the radius $R = 0.39$ fm for all hadrons. The dash-dotted lines show the results in the limit of ideal gas.

$N + \Delta + \pi$ matter and the acausal behavior appears even at larger n_B.

F. Role of quantum-statistical effects

Let us now discuss the applicability domain of the Boltzmann approximation (BA) which ignores possible effects of quantum (Bose and Fermi) statistics. It is well known [15] that, in the case of ideal gas, these effects become stronger at low temperatures and large chemical potentials. To include simultaneously the quantum-statistical and short-range repulsion effects, we apply below the procedure suggested in the excluded-volume model [5]. Only the case of equal hard-core radii for all hadrons ($R_i = R$) is considered.

The following equation for pressure is used in the EVM [7]:

$$P = \sum_i \widetilde{P}_i(\widetilde{\mu}_i, T), \tag{73}$$

where $\widetilde{P}_i(\widetilde{\mu}_i, T)$ is the partial pressure of ideal gas of the ith hadrons at temperature T and chemical potential $\widetilde{\mu}_i$. The relation connecting $\widetilde{\mu}_i$ with the real chemical potential μ_i reads

$$\widetilde{\mu}_i = \mu_i - bP, \tag{74}$$

where $b = 4v$ is the excluded-volume parameter introduced in Sec. II C. The expressions (73) and (74) give the implicit equation for P at given temperature and chemical potentials $\{\mu_i\}$. By using the conditions of chemical equilibrium (71) and strangeness neutrality (72), one can finally calculate pressure as well as partial densities $n_i = \partial P/\partial \mu_i$ at different μ_B and T.

Below we use the explicit relation [26]

$$\widetilde{P}_i(\widetilde{\mu}_i, T) = \frac{g_i}{6\pi^2} \int_{m_i}^{\infty} dE \left(E^2 - m_i^2\right)^{3/2} \times \left[\exp\left(\frac{E - \widetilde{\mu}_i}{T}\right) \pm 1\right]^{-1}. \tag{75}$$

The lower sign in Eq. (75) corresponds to mesons ($B_i = 0$),[11] and the upper sign to baryons ($B_i = 1$) or antibaryons ($B_i = -1$).

At sufficiently small μ_B one can represent the r.h.s. of Eq. (75) as a series in the fugacity $\exp(\widetilde{\mu}_i/T)$ [7]:

$$\widetilde{P}_i = \sum_{l=1}^{\infty} (\mp 1)^{l+1} \frac{T}{l} \phi_i\left(\frac{T}{l}\right) \exp\left(\frac{\widetilde{\mu}_i l}{T}\right). \tag{76}$$

Corresponding formulas in the BA are obtained if one retains only the first ($l = 1$) term in Eq. (76) or, equivalently, neglects the term (± 1) in the denominator of Eq. (75). Then we arrive at the approximate expression $\widetilde{P}_i \simeq T\phi_i(T) \exp(\widetilde{\mu}_i/T)$ which is the generalization of Eq. (24) for the case of multicomponent systems.

For a qualitative analysis, let us consider the nonrelativistic limit when $T \lesssim m_i$ for all hadronic species. In this case $\phi_i \propto T^{3/2} e^{-m_i/T}$ and one can see that the relative contribution of the $l = 2$ term in Eq. (76) is of the order of $e^{(\mu_i - m_i)/T}$ multiplied by the additional suppression factor $e^{-bP/T}$ due to the HSI. These estimates show that deviations from Boltzmann limit are relatively small if the conditions $\mu_i < m_i$ are satisfied. In particular, this means that the baryon chemical potential should not exceed the nucleon mass m_N.

Taking the parameter $b = 1\ \mathrm{fm}^3$ we have numerically solved Eqs. (73)–(75) in the temperature interval $0 < T < 250$ MeV. We take the same set of hadrons as in Sec. III E. We found that, indeed, relative magnitudes of quantum-statistical corrections to pressure and hadronic densities do not exceed several percent if $\mu_B < m_N$.

The situation is different for larger baryon chemical potentials. Note that at $\widetilde{\mu}_i > m_i$ the sum in Eq. (75) diverges at $l \to \infty$. In the considered region of μ_B the pressure of nonstrange baryons ($B_i = 1, S_i = 0$) does not vanish at zero temperature:

$$\widetilde{P}_i(\widetilde{\mu}_i, 0) = \frac{g_i}{6\pi^2} \int_{m_i}^{\widetilde{\mu}_i} dE \left(E^2 - m_i^2\right)^{3/2} \Theta(\widetilde{\mu}_i - m_i), \tag{77}$$

where $\Theta(x) = \frac{1}{2}[1 + \mathrm{sgn}(x)]$.

The results of our numerical calculations are presented in Figs. 15 and 16. By thick lines we show the pressure and baryon density as functions of temperature for several values of μ_B exceeding the nucleon mass. For comparison thin lines show the results in the Boltzmann approximation. One can see that, in the range $\mu_B = 1 - 1.4$ GeV, deviations from Boltzmann statistics are large at $T \lesssim 50$ MeV. However, they become relatively small at $T \gtrsim 100$ MeV. On the basis of this analysis we conclude that quantum-statistical corrections do not significantly modify the results of preceding sections, where we have mostly discussed temperatures above 100 MeV.

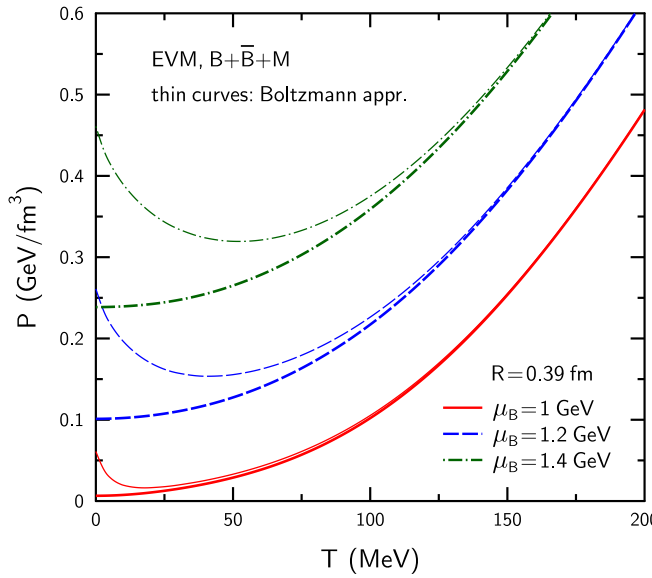

FIG. 15. (Color online) Pressure of hadronic gas as a function of temperature for different values of baryon chemical potential μ_B. The EVM calculations, assuming the radius $R = 0.39$ fm for all hadrons, are shown by thick lines. Thin curves show the results in the Boltzmann approximation.

[11] It is assumed that the conditions for Bose condensation of mesons, $\widetilde{\mu}_i \geqslant m_i$, are not satisfied (for details, see Ref. [7]).

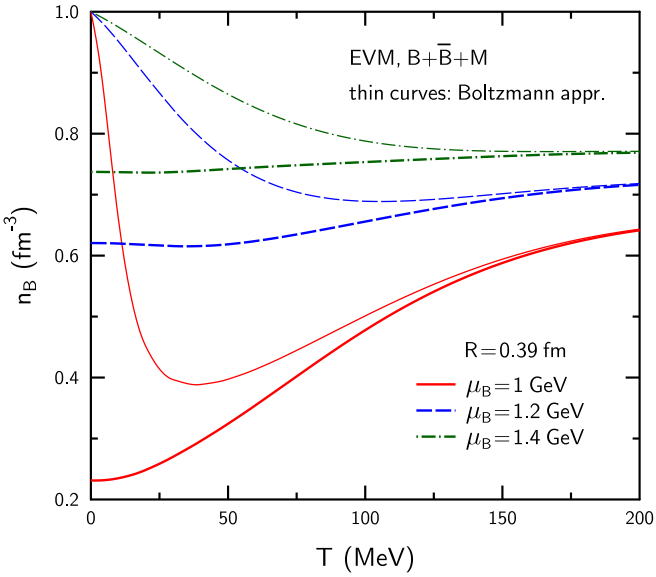

FIG. 16. (Color online) Same as Fig. 15 but for baryon density n_B.

One can see that slopes of thin lines in Fig. 15 are negative at small temperatures. Taking into account that $(\partial P/\partial T)_{\mu_B}$ equals the entropy density, we conclude that the third law of thermodynamics is violated in the BA (this is a well-known drawback of such approximation). Another unphysical prediction of the EVM with neglect of quantum-statistical effects is a universal value of the baryon density: $n_B \to b^{-1}$ at $T \to 0$ for all $\mu_B > m_N$.[12] According to Fig. 16, at $\mu_B \gtrsim 1.4$ GeV, baryon densities reach the values $n_B \gtrsim 0.8$ fm^{-3} which correspond to packing fractions $\eta \gtrsim 0.2$. As shown in Sec. II A, the EVM becomes unrealistic in this case.

In conclusion of this section we would like to note that our assumption of classical HSI of hadrons becomes questionable at low temperatures. Indeed, for this approach to be valid, the characteristic wavelengths of hadrons' relative motion should be smaller than the sum of their radii. This condition is certainly violated at $T \to 0$. Therefore, a real quantum description of hadronic interactions is required in this case. Some steps in this direction have been made in Refs. [6,27].

[12]It is interesting that the pressure in this limit remains finite, $P \to (\mu_B - m_N)/b$.

IV. CONCLUSIONS AND OUTLOOK

In this paper we investigated the EoS and sound velocities of one- and multicomponent hadronic systems with HSI. It is shown that widely used excluded-volume models become unrealistic at packing fractions exceeding about 0.2. We demonstrated that the Carnahan-Starling EoS is much softer and can be applied at much higher densities. Moreover, the sound velocity calculated for this EoS shows the acausal behavior only at very high baryon densities, presumably in the region of the quark-gluon phase transition. Comparing the sound velocities in hot and dense hadronic systems with different compositions of particles, we studied the sensitivity of the EoS of strongly interacting matter to the formation of mesons, antibaryons, and hadronic resonances.

We also estimated corrections to the EoS due to the quantum statistics. Our conclusion is that they are small unless the baryon chemical potential exceeds the nucleon mass and temperature is below 100 MeV. Therefore, these corrections can be safely neglected under conditions expected in heavy-ion collisions at laboratory energies exceeding approximately 1 GeV/nucleon.

In the future we are going to perform a more detailed analysis of hadronic mixtures with unequal radii of different particle species. Using the Carnahan–Starling EoS and the approach suggested in Ref. [7] we plan to investigate the sensitivity of the phase diagram of strongly interacting matter to finite sizes of hadrons. In this way one can construct a realistic EoS suitable for hydrodynamical modeling of heavy-ion collisions. In particular, one may perform calculations similar to those done in Refs. [28,29] to analyze possible signatures of the deconfinement phase transition at FAIR and NICA energies.

ACKNOWLEDGMENTS

The authors thank M. I. Gorenstein, C. Greiner, A. I. Ivanytskyi, and V. V. Sagun for useful discussions. We acknowledge partial financial support provided by the Helmholtz International Center for FAIR (Germany). Partial support from the grant NSH–932.2014.2 of the Russian Ministry of Education and Science is acknowledged by I.N.M. and L.M.S. K.A.B. acknowledges partial support from the program "On perspective fundamental research in high-energy and nuclear physics" launched by the Section of Nuclear Physics of the National Academy of Sciences of Ukraine.

[1] J. D. van der Waals, in *Nobel Lectures in Physics 1901–1921* (Elsevier, Amsterdam, 1967).
[2] J. P. Hansen and I. R. McDonald, *Theory of Simple Fluids* (Academic Press, Amsterdam, 2006).
[3] *Theory and Simulation of Hard Sphere Fluids and Related Systems*, Lect. Notes Phys. Vol. 753, edited by A. Mulero (Springer-Verlag, Berlin, 2008).
[4] J. Cleymans, K. Redlich, H. Satz, and E. Suhonen, Z. Phys. C: Part. Fields **33**, 151 (1986).
[5] D. H. Rischke, M. I. Gorenstein, H. Stöcker, and W. Greiner, Z. Phys. C: Part. Fields **51**, 485 (1991).
[6] R. Venugopalan and M. Prakash, Nucl. Phys. A **546**, 718 (1992).
[7] L. M. Satarov, M. N. Dmitriev, and I. N. Mishustin, Phys. Atom. Nucl. **72**, 1390 (2009) [Yad. Fiz. **72**, 1444 (2009)].

[8] K. A. Bugaev, Nucl. Phys. A **807**, 251 (2008).
[9] J. Steinheimer, S. Schramm, and H. Stöcker, J. Phys. G **38**, 035001 (2011).
[10] K. A. Bugaev, D. R. Oliinychenko, J. Cleymans, A. I. Ivanytskyi, I. N. Mishustin, E. G. Nikonov, and V. V. Sagun, Europhys. Lett. **104**, 22002 (2013).
[11] D. R. Oliinychenko, K. A. Bugaev, and A. S. Sorin, Ukr. J. Phys. **58**, 211 (2013).
[12] S. Kagiyama, A. Minaka, and A. Nakamura, Prog. Theor. Phys. **89**, 1227 (1993).
[13] C. P. Singh, B. K. Patra, and K. K. Singh, Phys. Lett. B **387**, 680 (1996).
[14] M. I. Gorenstein, Phys. Rev. C **86**, 044907 (2012).
[15] L. D. Landau and E. M. Lifshitz, *Statistical Physics* (Pergamon Press, Oxford, 1980).
[16] N. F. Carnahan and K. E. Starling, J. Chem. Phys. **51**, 635 (1969).
[17] L. D. Landau and E. M. Lifshitz, *Fluid Mechanics* (Pergamon Press, Oxford, 1987).
[18] A. Mulero, C. A. Faúndez, and F. Cuadros, Mol. Phys. **97**, 453 (1999).
[19] Y. Aoki *et al.*, J. High Energy Phys. 06 (2009) 088.
[20] A. Bazavov *et al.* (HotQCD Collaboration), Phys. Rev. D **85**, 054503 (2012).
[21] B. J. Alder, J. Chem. Phys. **23**, 263 (1955).
[22] V. M. Galitsky and I. N. Mishustin, Sov. J. Nucl. Phys. **29**, 181 (1979) [Yad. Fiz. **29**, 363 (1979)].
[23] S. Weinberg, Astrophys. J. **168**, 175 (1971).
[24] Ya. B. Zeldovich, Sov. Phys. JETP **41**, 1143 (1962) [Zh. Eksp. Teor. Phys. **41**, 1609 (1961)].
[25] J. Cleymans, H. Oeschler, K. Redlich, and S. Wheaton, Phys. Lett. B **615**, 50 (2005).
[26] G. D. Yen, M. I. Gorenstein, W. Greiner, and S. N. Yang, Phys. Rev. C **56**, 2210 (1997).
[27] A. Kostyuk, M. Gorenstein, H. Stöcker, and W. Greiner, Phys. Rev. C **63**, 044901 (2001).
[28] A. V. Merdeev, L. M. Satarov, and I. N. Mishustin, Phys. Rev. C **84**, 014907 (2011).
[29] K. A. Bugaev, A. I. Ivanytskyi, D. R. Oliinychenko, V. V. Sagun, I. N. Mishustin, D. H. Rischke, L. M. Satarov, and G. M. Zinovjev, Phys. Part. Nucl. Lett. **12**, 238 (2015).